Journal of Power Sources 195 (2010) 6532–6538

Contents lists available at ScienceDirect

Journal of Power Sources

journal homepage: www.elsevier.com/locate/jpowsour

High efficiency chemical energy conversion system based on a methane catalytic decomposition reaction and two fuel cells. Part II. Exergy analysis

Qinghua Liu[a], Ye Tian[a], Hongjiao Li[a], Lijun Jia[a], Chun Xia[a], Levi T. Thompson[b], Yongdan Li[a,*]

[a] Tianjin Key Laboratory of Catalysis Science and Technology and State Key Laboratory for Chemical Engineering (Tianjin University), School of Chemical Engineering, Tianjin University, Tianjin 300072, China
[b] Department of Chemical Engineering, University of Michigan, Ann Arbor, MI 48109-2136, United States

ARTICLE INFO

Article history:
Received 23 March 2010
Received in revised form 14 April 2010
Accepted 14 April 2010
Available online 21 April 2010

Keywords:
Methane catalytic decomposition
Direct carbon fuel cell
Solid oxide fuel cell
Gas turbine
Combined power and heat system
Exergy

ABSTRACT

A methane catalytic decomposition reactor-direct carbon fuel cell-internal reforming solid oxide fuel cell (MCDR-DCFC-IRSOFC) energy system is highly efficient for converting the chemical energy of methane into electrical energy. A gas turbine cycle is also used to output more power from the thermal energy generated in the IRSOFC. In part I of this work, models of the fuel cells and the system are proposed and validated. In this part, exergy conservation analysis is carried out based on the developed electrochemical and thermodynamic models. The ratio of the exergy destruction of each unit is examined. The results show that the electrical exergy efficiency of 68.24% is achieved with the system. The possibility of further recovery of the waste heat is discussed and the combined power-heat exergy efficiency is over 80%.

1. Introduction

Methane catalytic decomposition (MCD) is an attractive route for the production of hydrogen due to its simplicity in comparison to steam reforming and the absence of CO_x by-product [1–7]. The carbon produced using this process is filamentous [8,9] and can be used as the fuel of a direct carbon fuel cell (DCFC) [10]. In part I of this work, a high efficiency energy conversion system integrating a MCD reactor (MCDR) [11], DCFC [12], IRSOFC [13,14] and GTs was designed and validated with operating models for the individual parts and the integrated system.

A useful metric for characterizing the utilization of energy for a system is the exergy [15]. Different from a simple energy analysis which deals with the quantity of energy, an exergy analysis identifies the location and magnitude of the useful energy destruction in the system and suggests improvements of the system efficiency, thus takes to account both the quantity and quality of energy. Extensive examinations have been conducted on the energy and exergy of SOFC–GT integrated systems [16–18]. Panopoulos et al. performed an exergy analysis for a high temperature SOFC integrated with an autothermal biomass gasification unit [19,20]. The electrical exergy efficiency is 32% and the combined heat-power exergy efficiency is 35%. Li et al. carried out an exergy conservation analysis for a high efficiency power generation process using natural gas, integrating a MCDR, DCFC and proton exchange membrane fuel cell (PEMFC) [10]. The results show that 76% electrical exergy efficiency can be reached.

Work described in this paper focuses on an exergy analysis of the integrated energy system described in part I. The energy and exergy destructions of each component are investigated, and the overall system exergy efficiency is determined as well as an exergy flow diagram is given.

2. System layout

The flow sheet for the proposed system, with numbered streams, is presented in Fig. 1. The major components include a MCDR, a IRSOFC, a DCFC with molten carbonate electrolytes, a catalytic afterburner (AB), an air compressor (AC), a heat recovery steam generator (HRSG), two gas turbines (one (GT) is used to drive the air compressor, and the other one (PT) is used to generate power), a carbon dioxide–air mixer (M1), a steam–gaseous fuel mixer (M2), a methane–DCFC exhaust heat exchanger (HX1), an air–DCFC exhaust heat exchanger (HX2), a gaseous fuel–AB exhaust heat exchanger (HX3), and a pump (P). The invertors are not shown in this figure.

In this system, methane is preheated in the HX1 with the DCFC exhaust gas, which are also used to preheat the DCFC inlet air in

* Corresponding author. Tel.: +86 22 27405613; fax: +86 22 27405243.
E-mail address: ydli@tju.edu.cn (Y. Li).

0378-7753/$ – see front matter © 2010 Elsevier B.V. All rights reserved.
doi:10.1016/j.jpowsour.2010.04.048

Nomenclature

A_i	thermal capacity constant of species i ($J\,s^{-1}$)
B_i	thermal capacity constant of species i ($J\,s^{-1}$)
C_i	thermal capacity constant of species i (K^2)
D_i	thermal capacity constant of species i (K^{-2})
E_{ch}	chemical exergy (J)
E_{ph}	physical exergy (J)
Ex	exergy (J)
Ex_d	exergy destruction (J)
e^o_{ch}	mole chemical exergy at standard state ($J\,mol^{-1}$)
h_i	mole enthalpy of species i ($J\,mol^{-1}$)
h_o	mole enthalpy at standard state ($J\,mol^{-1}$)
m	mass flow rate ($kg\,s^{-1}$)
n_i	mole flow rate of species i ($mol\,s^{-1}$)
P	power (W)
Q	heat (J)
R	gas constant ($8.314\,J\,mol\,K^{-1}$)
s_i	mole entropy of species i ($J\,mol^{-1}\,K^{-1}$)
s_o	mole entropy at standard state ($J\,mol^{-1}\,K^{-1}$)
T	temperature (K)
x_i	mole fraction of species i (mol%)
W	work (J)

Greek letters

$\eta_{Ex,c}$	combined heat-power exergy efficiency (%)
$\eta_{Ex,el}$	electric exergy efficiency (%)

Subscripts

cold	cold stream
hot	hot stream
in	inlet
out	outlet

the HX2. The preheated CH_4 fuel is fed into the MCDR and decomposed to H_2 and carbon. The carbon materials are absorbed and transported by a molten carbonate stream into the DCFC anode, and consumed electrochemically there to release electrons and produce CO_2. A fraction of CO_2 (66.7 mol%) is sent to the DCFC cathode to regenerate the carbonate after mixing with air (CO_2/O_2 ratio 2:1) in M1. The rest CO_2 (33.3 mol%) is used to preheat air and CH_4. The gaseous products containing H_2 generated in the MCDR and unconverted CH_4 are fed into the IRSOFC anode after mixing with steam in the M2. The internal reforming reaction occurs in the IRSOFC anode compartment. Methane is converted into H_2. Air is compressed in the AC and preheated in the HX3 and fed into the IRSOFC cathode. The SOFC cell reaction is exothermic, and the heat generated is partially used to drive the internal reforming reaction. The O_2 depleted air and the unreacted gaseous fuel are burned in the AB. The exhaust emitted from the AB can be further utilized to offer shaft work for the air compress in the GT and generate power in the GT. Finally, it is used to preheat air entering the IRSOFC cathode and generate steam in the HRSG, respectively. It is assumed that there is no heat transfer with the surroundings in above processes. All operating parameters used are listed in Table 1.

3. Exergy analysis

3.1. Methodologies

Exergy is the maximum work obtainable when a substance or a material stream is brought to a state of thermodynamic equilibrium through a serious of reversible processes [21]. Exergy analysis of a process is the assessment of the conservation of mass and energy with the second law of thermodynamics. The exergy is often used to assess the work potential for a thermal system, define the irreversible losses, and optimize the utilization of the energy.

In this work, assuming negligible kinetic and potential exergies, the total exergy associated with a material stream is the sum of physical exergy and chemical exergy:

$$Ex = E_{ph} + E_{ch} \tag{1}$$

The physical exergy is the work obtainable by taking the material stream to the standard environment state through a reversible physical process. It is associated with the temperature and the pressure of the material stream and can be described as follows:

$$E_{ph} = \sum_i [n_i(h_i - h_o) - n_i T_o(s_i - s_o)] \tag{2}$$

where n_i denotes the mole flow of component i, h_i and s_i are the mole enthalpy and mole entropy of component i, respectively, h_o and s_o are the mole enthalpy and mole entropy of the component i at standard state, respectively.

The chemical exergy is the work obtainable by taking the material stream at T_o and P_o to the state of thermodynamic equilibrium with the datum level components of the environment. It is associated with the initial chemical composition of a material stream. The chemical exergy of a gaseous mixture is determined as follows:

$$E_{ch} = \sum_i n_i \sum_i (x_i e^o_{ch} + RT_o \ln x_i) \tag{3}$$

where x_i is the mole fraction of component i in the mixture, and e^o_{ch} is the mole chemical exergy at standard state. These values are given in Table 2 [16].

Heat, Q, cannot be converted into work or exergy completely because the conversion is governed by the Carnot efficiency which can be calculated as follows,

$$Ex_{Q,T} = Q\left(1 - \frac{T_o}{T}\right) \tag{4}$$

where T is the temperature at which Q is available. Since the power output can be totally transferred to work, the value of the exergy of the electric work is equal to that of the electric work itself.

At the temperatures and pressures used in this analysis, the gases are assumed to obey the ideal gas law. The enthalpies and entropies of all substances are temperature-dependent and determined as follows:

$$h_i = A_i T + \frac{B_i}{2}T - C_i T^{-1} + \frac{D_i}{3}T^3 \tag{5}$$

$$s_i = A_i \ln\ T + B_i T - \frac{C_i}{2}T^{-1} + \frac{D_i}{2}T^2 \tag{6}$$

The coefficients used in this work are given in Table 3 [22].

3.2. Methane catalytic decomposition reactor

In the MCDR, CH_4 is catalytically decomposed into H_2 and carbon. The mass balance equation is:

$$m_2 = m_3 + m_{11} \tag{7}$$

The energy balance is:

$$\sum_i n_{i,2}h_{i,2} - \sum_j n_{j,3}h_{j,3} - \sum_j n_{j,11}h_{j,11} + Q_M = 0 \tag{8}$$

The exergy balance is given by:

$$Ex_2 - Ex_3 - Ex_{11} + \left(1 - \frac{T_o}{T_{MCDR}}\right)Q_M - Ex_{d,MCDR} = 0 \tag{9}$$

where T_{MCDR} is the operating temperature for the MCDR and $Ex_{d,MCDR}$ is the exergy destruction in this unit.

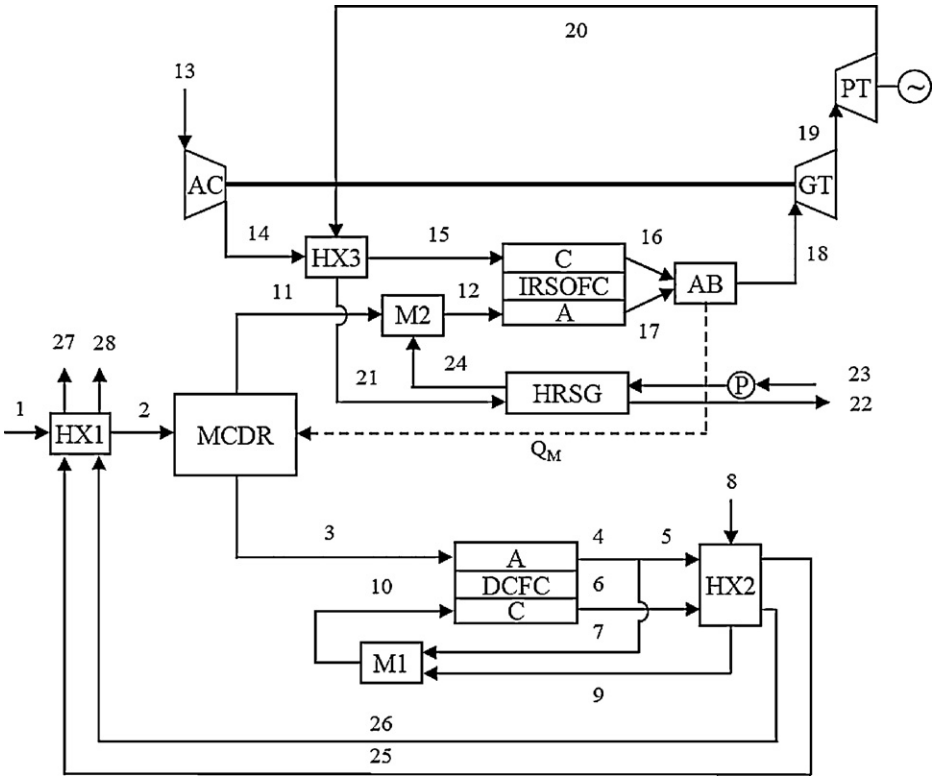

Fig. 1. A schematic diagram of the proposed system.

Table 1
Operating parameters.

Parameters	Values
MCDR	
Operating temperature (K)	1073–1273
Methane inlet molar flow rate ($mol\,s^{-1}$)	1.0
DCFC	
Operating temperature (K)	873–1073
Operating pressure (atm)	1.0
Fuel utilization (%)	100
Air utilization (%)	50
CO_2 utilization in the cathode (%)	100
IRSOFC	
Operating temperature (K)	1073–1273
Operating pressure (atm)	1.0
Fuel utilization (%)	80.00
Air utilization (%)	30.00
Steam to carbon ratio	2.2:1.0
Other components	
AC efficiency (%)	81
GT efficiency (%)	84
PT efficiency (%)	89
HRSG efficiency (%)	80
Heat exchanger effectiveness (%)	98
Catalytic afterburner efficiency (%)	100

Table 2
Mole chemical exergies at standard state.

Species	E_x ($J\,mol^{-1}$)
C	410,260
CH_4 (g)	83,160
CO_2	19,870
H_2	236,100
H_2O (g)	9500
H_2O (l)	900
N_2	720
O_2	3970

Table 3
Coefficients for Eqs. (5) and (6).

Species	A_i	B_i (K^{-1})	C_i (K^2)	D_i (K^{-2})
C	1.09E−01	3.89E+02	−1.48E+05	−1.74E−07
CH_4	2.73E00	9.63E−02	5.90E+05	−2.68E−05
CO_2	2.22E+01	5.62E−02	1.05E+04	2.25E−05
H_2	2.59E+01	4.84E−03	1.58E+05	−3.72E−07
H_2O (g)	2.19E+01	2.26E−02	8.49E+05	−4.00E−06
H_2O (l)	1.43E+01	5.50E−03	1.40E+05	5.98E−06
N_2	2.26E+01	1.32E+01	3.13E+05	−3.39E−06
O_2	3.10E+01	4.19E−03	−2.86E+05	3.85E−07

3.3. Direct carbon fuel cell

In this dual fuel cell energy system, the DCFC is used to convert the carbon formed during the methane catalytic decomposition into power and CO_2.

The mass balance equation is:

$$m_3 + m_{10} = m_4 + m_6 \tag{10}$$

The energy balance is:

$$\sum_i n_{i,3}h_{i,3} + \sum_i n_{i,10}h_{i,10} - \sum_j n_{j,4}h_{j,4} - \sum_j n_{j,6}h_{j,6} - Q_{DCFC} - W_{DCFC} = 0 \tag{11}$$

W_{DCFC} and Q_{DCFC} are the electric work output and the waste heat for the DCFC, respectively.

The exergy balance is described as:

$$Ex_3 + Ex_{10} - Ex_4 - Ex_6 - \left(1 - \frac{T_o}{T_{DCFC}}\right) Q_{DCFC} - W_{DCFC} - Ex_{d,DCFC} = 0 \tag{12}$$

where T_{DCFC} is the operating temperature and $Ex_{d,DCFC}$ is the exergy destruction in the device.

3.4. Internal reforming solid oxide fuel cell

A series of reactions including methane–steam reforming, water–gas shift, and electrode semi-reactions occur inside the IRSOFC.

The mass balance is:

$$m_{12} + m_{15} = m_{16} + m_{17} \tag{13}$$

The energy balance is:

$$\sum_i n_{i,12}h_{i,12} + \sum_i n_{i,15}h_{i,15} - \sum_j n_{j,16}h_{j,16} - \sum_j n_{j,17}h_{j,17} - Q_{SOFC} - W_{SOFC} = 0 \tag{14}$$

W_{SOFC} and Q_{SOFC} are the IRSOFC electric work output and waste heat, respectively.

The exergy balance is given by:

$$Ex_{12} + Ex_{15} - Ex_{16} - Ex_{17} - \left(1 - \frac{T_o}{T_{SOFC}}\right) Q_{SOFC} - W_{SOFC} - Ex_{d,SOFC} = 0 \tag{15}$$

where T_{SOFC} is the operating temperature of IRSOFC, and $Ex_{d,SOFC}$ is the exergy destruction in IRSOFC.

3.5. Gas turbines

The work output, outlet temperature and exergy destructions both for the GT and the PT can be determined using the following equations.

$$m_{in} = m_{out} \tag{16}$$

$$\sum_i n_{i,in}h_{i,in} - \sum_j n_{j,out}h_{j,out} - W_{GT} = 0 \tag{17-a}$$

or

$$\sum_i n_{i,in}h_{i,in} - \sum_j n_{j,out}h_{j,out} - W_{PT} = 0 \tag{17-b}$$

$$Ex_{in} - Ex_{out} - W_{GT} - Ex_{d,GT} = 0 \tag{18-a}$$

or

$$Ex_{in} - Ex_{out} - W_{GT} - Ex_{d,PT} = 0 \tag{18-b}$$

where $Ex_{d,GT}$ and $Ex_{d,PT}$ are the exergy destruction in the GT and the PT, respectively.

3.6. Catalytic afterburner

In the catalytic afterburner, the SOFC anode fuel depleted exhaust is completely oxidized using the cathode oxygen depleted air. The high temperature flue gas is used to preheat the inlet fuel and air.

The mass balance is:

$$m_{16} + m_{17} = m_{18} \tag{19}$$

The energy balance is:

$$\sum_i n_{i,16}h_{i,16} + \sum_i n_{i,17}h_{i,17} - \sum_j n_{j,18}h_{j,18} - Q_M = 0 \tag{20}$$

The exergy balance is:

$$Ex_{16} + Ex_{17} - Ex_{18} - \left(1 - \frac{T_o}{T_{AB}}\right) Q_M - Ex_{d,AB} = 0 \tag{21}$$

where T_{AB} is the outlet temperature of the catalytic afterburner.

3.7. Heat exchangers and HRSG

There are three heat exchangers used in this system. Since no chemical reactions occur inside, the outlet temperature and the exergy destruction for each can be determined using the following three equations.

$$m_{hot,in} + m_{cold,in} = m_{hot,out} + m_{cold,out} \tag{22}$$

$$\sum_i n_{i,hot,in}h_{i,hot,in} + \sum_i n_{i,cold,in}h_{i,cold,in} - \sum_j n_{j,hot,out}h_{j,hot,out} - \sum_j n_{j,cold,out}h_{j,cold,out} = 0 \tag{23}$$

$$Ex_{hot,in} + Ex_{cold,in} - Ex_{hot,out} - Ex_{cold,out} - Ex_{d,HX} = 0 \tag{24}$$

where $Ex_{d,HX}$ is the exergy destruction in the heat exchanger. The mass balance, energy balance and exergy balance for the HRSG are same as that of the heat exchanger except for the consideration of the phase change of water.

3.8. Mixers

There are two mixers in the system. For mixer 1, the mass balance is:

$$m_7 + m_9 = m_{10} \tag{25}$$

The energy balance is:

$$\sum_i n_{i,7}h_{i,7} + \sum_i n_{i,9}h_{i,10} - \sum_j n_{j,10}h_{j,10} = 0 \tag{26}$$

The exergy balance is:

$$Ex_7 + Ex_9 - Ex_{10} - Ex_{d,M1} = 0 \tag{27}$$

where $Ex_{d,M1}$ is the exergy destruction of mixer 1. Analogous equations can be used to determine the mass, energy and exergy balances for mixer 2.

3.9. Analysis of the integrated system

The model for the system was developed using the commercial software package, Matlab. Solutions for subroutines for each component are carried out sequentially, while the inlet and outlet temperatures for the MCDR, SOFC, DCFC, GT, PT, and AB are solved iteratively.

The electrical exergy efficiency of the overall integrated system is defined as the ratio of the power output from DCFC, SOFC, and PT to the input CH_4 exergy:

$$\eta_{Ex,el} = \frac{W_{DCFC} + W_{SOFC} + W_{PT}}{Ex_{CH_4}} \tag{28}$$

The combined heat-power exergy efficiency is defined as:

$$\eta_{Ex,c} = \frac{W_{DCFC} + W_{SOFC} + W_{PT} + Ex_{ex,22} + Ex_{ex,27} + Ex_{ex,28}}{Ex_{CH_4}} \tag{29}$$

where $Ex_{ex,22}$, $Ex_{ex,27}$, and $Ex_{ex,28}$ are the exergies of the heat contained in the exhausts emitted following from the nodes 22, 27 and 28, respectively.

Table 4
Mass and thermodynamic properties for each node.

Node	T/K	C	CH_4	CO_2	H_2	H_2O (g)	O_2	N_2	H_2O (l)	H ($J\,s^{-1}$)	S ($J\,s^{-1}\,K^{-1}$)	A ($J\,s^{-1}$)	$E_{x,ph}$ ($J\,s^{-1}$)	$E_{x,ch}$ ($J\,s^{-1}$)	E_x ($J\,s^{-1}$)
1	298	–	1.0	–	–	–	–	–	–	0	0	0	0	831,650	831,650
2	775	–	1.0	–	–	–	–	–	–	23,242	44	13,268	9973	831,650	841,624
3	1073	0.8	–	–	–	–	–	–	–	10,727	16	4844	5882	328,208	334,090
4	1153	–	–	2.4	–	–	–	–	–	10,0994	152	45,523	55,471	47,688	103,159
5	1153	–	–	0.8	–	–	–	–	–	33,664	50	15,174	18,490	15,896	34,386
6	1153	–	–	–	–	–	0.8	6.4	–	192,568	299	89,259	103,308	1558	104,866
7	1153	–	–	1.6	–	–	–	–	–	67,329	101	30,348	36,980	31,792	68,773
8	298	–	–	–	–	–	1.6	6.4	–	0	0	0	0	0	0
9	775	––	–	–	–	–	1.6	6.4	–	115,672	230	68,619	47,052	0	47,052
10	871	–	–	1.6	–	–	1.6	6.4	–	183,136	337	100,654	82,481	22,107	104,588
11	1073	–	0.2	–	1.6	–	–	–	–	45,323	73	21,873	23,450	301,408	565,984
12	1000	–	0.2	–	1.6	–	0.44	–	–	52,089	88	26,286	25,802	543,962	569,765
13	298	–	–	–	–	–	3.09	12.37	–	0	0	0	0	0	0
14	443	–	–	–	–	–	3.09	12.37	–	51,513	146	43,537	7976	0	7976
15	800	–	–	0.2	–	–	3.09	12.37	–	235,854	460	137,292	98,562	0	98,562
16	1154	–	–	0.2	–	–	2.17	12.37	––	389,812	605	180,660	209,152	2337	211,490
17	1154		0.02	0.18	0.46	1.94	–	–	–	83,239	127	38,162	45076.2	175,511	220,587
18	1433	–	–	0.2	–	2.44	1.87	12.37	–	643,980	865	258,148	385,832	45,448	431,280
19	1320	–	–	0.2	–	2.44	1.87	12.37	–	573,781	814	242,936	330,845	45,448	376,293
20	1109	–	–	0.2	–	2.44	1.87	12.37	–	445,985	709	211,507	234,478	45,448	279,926
21	770	–	–	0.2	–	2.44	1.87	12.37	–	249,896	498	148,732	101,164	45,448	146,612
22	730	–	–	0.2	–	2.44	1.87	12.37	–	227,702	469	139,913	87,789	45,448	133,238,
23	298	–	–	–	–	–	–	–	0.44	0	0	0	0	396	396
24	732	–	–	–	–	0.44	–	–	–	6770	13	4142	2628	4180	6808
25	795	–	–	0.8	–	–	–	–	–	18120	34	10,373	7747	15,896	23,643
26	795	–	–	–	–	–	0.8	6.4	–	108,011	211	63,139	44,871	1558	46,429
27	706	–	–	0.8	–	–		–	–	14,478	29	8925	5552	15,896	21,448
28	706	–	–	–	–	–	0.8	6.4	–	87,945	208	62,195	25,750	1558	27,308

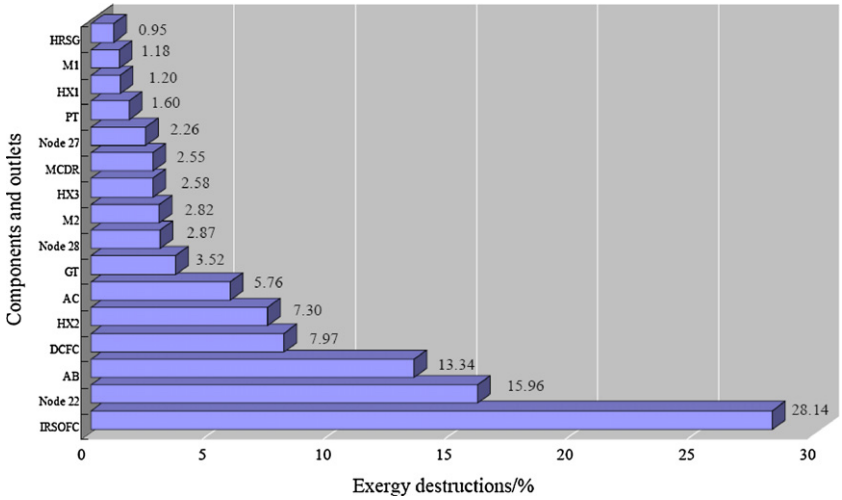

Fig. 2. Exergy destructions in each component and outlet.

Additional assumptions are listed as follows:

- Steady state operation for all components with negligible friction loss.
- All gases, e.g. CH_4, CO, CO_2, H_2O, H_2, N_2, and O_2, are ideal gas. The air contains 21 mol% O_2 and 79 mol% N_2.
- The operation pressure of MCDR, DCFC is 1 atm with negligible pressure loss.

4. Results and discussion

4.1. Mass and energy balances

Based on the mass balance and the energy balance equations, the compositions, flow rates, and temperature of all material streams can be determined for each node. The results are summarized in Table 4. Since the temperature of carbon exiting the MCDR is 1073 K (as high as DCFC operating temperature), the carbon material is fed directly into the DCFC anode without preheating. Moreover, the MCD process is O_2-free, therefore there no O_2 and CO in the carbon material. The MCD process is favorable for integration with the DCFC.

The exhaust heat produced by the system can be further utilized. As presented in Table 4, at node 22, the high temperature gaseous mixture contains CO_2, N_2, O_2 and steam, and a significant amount of heat. The composition is affected by the fuel and oxygen utilization, and the steam to carbon ratio for the SOFC. It can be used for power and heat cogeneration through heat recovery. At node 28, the high temperature O_2 depleted air can be used for power and heat cogeneration together with the gaseous mixture from node 22, while the gaseous stream at node 27 is from the DCFC anode and contains only CO_2. The high temperature CO_2 can also be used for heat generation. This CO_2 can be further utilized to produce beverages, fertilizer, organic materials and as a preservative agent.

4.2. Exergy balance and efficiencies

The exergies of each node are given in Table 4. According to the energy and exergy balances, the electrical exergy efficiency for the proposed system is 68.24%. If the heat recovery process is incorporated for waste heat utilization, an additional electrical efficiency of at least 12% can be achieved. It should be noted that the efficiency of the system is strongly dependent on the operating conditions of the DCFC and IRSOFC. It is assumed that the operating voltages of DCFC and IRSOFC are around 6.5 V and 7.5 V, respectively.

Fig. 2 presents the exergy destructions for all the components and exhausts considered. The IRSOFC contributes the major exergy destruction due to the irreversibility of multiple reactions including the reforming and electrochemical reactions and the polarization losses. Another significant exergy destruction source is the catalytic afterburner caused by irreversible combustion reactions. Compared to the IRSOFC, the DCFC has less exergy destruction owing to its simple cell reactions. The recovery of the waste heat of emission at node 22 is limited by the Carnot efficiency, leading to large amount of exergy destruction. The high temperature exhausts are utilized to preheat the atmospheric temperature air in HX2. Hence, relatively large exergy destructions occur due to the large temperature difference.

An exergy flow diagram in which the exergy values are normalized by the chemical exergy of CH_4 is presented in Fig. 3. In this case, fuel utilization for the DCFC and SOFC are 100% and 80%, respectively. For each control volume in the system proposed, the input exergies are balanced by the outlet exergies plus the exergy

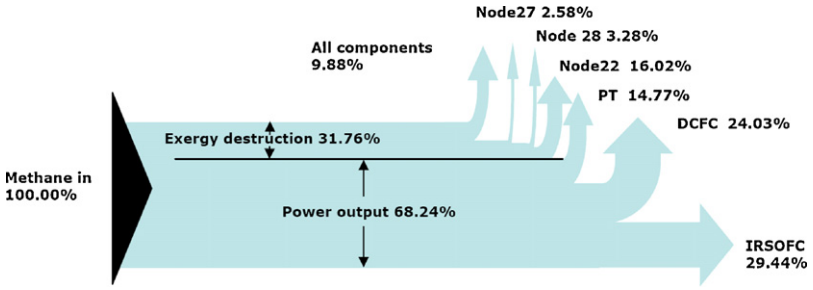

Fig. 3. Exergy flow for the proposed system.

destructions. The total exergy of the exhaust emitted in node 22, 27 and 28 is 21.88%. As mentioned above, this can be recovered partially through the heat recovery process to provide thermal energy for resident and industrial utilization.

5. Conclusions

An energy system integrating a MCDR, DCFC, IRSOFC, and GTs was analyzed with exergy conservation as the target function. This system appears to be very promising for high efficiency combined heat and power generation.

This system is autothermal and does not require external heat input because all heat requirements are satisfied by the DCFC and catalytic exhaust afterburner. The electrical exergy efficiency of the proposed system is 68.24%. The IRSOFC contribute to the major exergy destruction due to its complex reactions in the anode. The exergy destruction of DCFC is close to one third of that of IRSOFC. The exhausts contain 21.88% of exegy of the inlet fuel, a part of which can be recovered with recuperation units that would result in further increases in the combined power-heat system and the overall exergy efficiency can be over 80%. This combined technology system is not being studied from an economic viewpoint here and this paper is only a theoretical exergy analysis based on postulated theoretical parameters. A further study of engineering economic analysis of the system is strongly recommended.

Acknowledgements

This work has been supported by the Natural Science Foundation of China under contract numbers 20425619 and 20736007. The work has been also supported by the Program of Introducing Talents to the University Disciplines under file number B06006, and the Program for Changjiang Scholars and Innovative Research Teams in Universities under file number IRT 0641.

References

[1] Y.D. Li, J.L. Chen, Y.N. Qin, L. Chang, Energy Fuels 14 (2000) 1188–1194.
[2] M. Steinberg, H.C. Cheng, Int. J. Hydrogen Energy 14 (1993) 797–820.
[3] N.Z. Muradov, Int. J. Hydrogen Energy 18 (1993) 211–215.
[4] J.L. Chen, X.M. Li, Y.D. Li, Y.N. Qin, Chem. Lett. 32 (2003) 424–425.
[5] J.L. Chen, Y.H. Qiao, Y.D. Li, Appl. Catal. A 337 (2008) 148–154.
[6] J.L. Chen, Q. Ma, Thomas E. Rufford, Y.D. Li, Z.H. Zhu, Appl. Catal. A 362 (2009) 1–7.
[7] D.X. Li, J.L. Chen, Y.D. Li, Int. J. Hydrogen Energy 34 (2009) 299–307.
[8] Y.D. Li, J.L. Chen, L. Chang, Appl. Catal. A 163 (1997) 45–57.
[9] Y.D. Li, J.L. Chen, L. Chang, Y.N. Qin, J. Catal. 178 (1998) 76–83.
[10] Y.D. Li, R. Zhang, J.L. Chen, X.M. Li, A highly efficient power generation process from natural gas: An exergy analysis, in: 2th European Hydrogen Energy Conference, Zaragoza, Spain, November, 2005, 2005.
[11] W.H. Qian, T. Liu, Z.W. Wang, F. Wei, Z.F. Li, G.H. Luo, Y.D. Li, Appl. Catal. A 260 (2004) 223–228.
[12] Q.H. Liu, Y. Tian, C. Xia, L.T. Thompson, B. Liang, Y.D. Li, J. Power Sources 185 (2008) 1022–1029.
[13] P. Aguiar, C.S. Adjiman, N.P. Brandon, J. Power Sources 138 (2004) 120–136.
[14] P. Aguiar, C.S. Adjiman, N.P. Brandon, J. Power Sources 147 (2005) 136–147.
[15] A. Kazim, Energy Covers. Manage. 45 (2004) 1949–1961.
[16] P.G. Bavarsad, Int. J. Hydrogen Energy 32 (2007) 4591–4599.
[17] M. Granovskii, I. Dincer, M.A. Rosen, J. Power Sources 165 (2007) 307–314.
[18] F. Calise, A. Palombo, L. Vanoli, J. Power Sources 158 (2006) 225–244.
[19] K.D. Panopoulos, L.E. Fryda, J. Karl, S. Poulou, E. Kakaras, J. Power Sources 159 (2006) 570–585.
[20] K.D. Panopoulos, L.E. Fryda, J. Karl, S. Poulou, E. Kakaras, J. Power Sources 159 (2006) 586–594.
[21] J. Szargut, D.R. Morris, F.R. Steward, Exergy Analysis of Thermal, Chemical, and Metallurgical Processes, 1988, Hemisphere Publishing Corporation, New York, U.S.
[22] .W.J. Chase, J. Phys. Chem. Ref. Data, Monograph No. 9, "NIST-JANAF Thermochemical Tables", 1998.